Hindawi
Advances in Condensed Matter Physics
Volume 2023, Article ID 6773192, 8 pages
https://doi.org/10.1155/2023/6773192

Research Article

Dispersion Properties of Surface Waves Decaying in Red-Shifted and Blue-Shifted Gaps in Photonic Hypercrystals

Hasnain Haider and Munazza Zulfiqar Ali

University of the Punjab Lahore, Lahore, Pakistan

Correspondence should be addressed to Hasnain Haider; ha7nain@gmail.com

Received 29 June 2023; Revised 16 August 2023; Accepted 1 September 2023; Published 7 October 2023

Academic Editor: Upendra Kumar

The dispersion characteristics of surface waves for transverse electric and magnetic polarization modes of photonic hypercrystals (PHC) are theoretically explored. PHC are composed of a dielectric and hyperbolic metamaterial (HMM) with thin layers of both metal and dielectric surface waves that decay inside red-shifted gaps have a negative group velocity, whereas surface waves that decay inside traditional blue-shifted gaps have more typical characteristics. Curve plotting is used to elucidate on how these surface waves depend on several other structural properties such as filling factor, widths of HMM and dielectric, frequency range and angle of incidence etc.

1. Introduction

In recent years, the periodic multilayer structures have attracted great interest of researchers. The theoretical existence of new materials that can change the collaboration between light and matter has been anticipated, one of such is the photonic hypercrystal (PHC) [1]. It is the artificial optical media that consolidates the properties of photonic crystals (PC) [2] and hyperbolic metamaterials (HMMs) [3]. PC is a periodic structure in an optical medium showing bands and gaps [4]. These have captured considerations because of control on the flow of light on a very small length scale but have bandwidth constraints. One-dimensional periodic structures in the form of thin film stacks have been studied for many years, however three-dimensional photonic crystal was first proposed by Yablonovitch [5] and John [6] in 1987. Comparably, metamaterials (MM) [7] are artificial materials that have superior and surprising properties, yet have poor light emission rate. HMM named so due to its isofrequency hyperboloidal dispersion in wavevector space, is a hybrid material that behaves as a metal for wave propagation from one side and as a dielectric from the perpendicular side. The field of HMM started from hypothetical instincts that found in plasmonics [8], interesting features such as a tunable and broadband response makes such media a remarkable tool of nanophotonics, and can accelerate the progress from electronic to optical correspondences, both on a classical and on a quantum level [9]. The dielectric functions for HMM are described by tensor in terms of parallel ε_τ and perpendicular ε_n to the interface. These uniaxial crystals represent a dielectric media when $(\varepsilon_n > 0, \varepsilon_\tau > 0)$, metal $(\varepsilon_n < 0, \varepsilon_\tau < 0)$ and HMM $(\varepsilon_n \times \varepsilon_\tau < 0)$. HMMs have interesting and unique properties and applications due to its dielectric function variations in quantum nanophotonics [10], Dyakonov plasmonics [11], and super-Planckian emission control [12]. When PC and HMM are combined into PHC, the emission rate and bandwidth become higher, hence novel attributes can be promised. PHC is designed by the introduction of a systematic varieties in HMMs [13], by setting the size of such crystals lesser than the wavelength of free space $(\Lambda \ll \lambda_0)$ not too smaller than the unit size of HMM $(\Lambda \gg d_H)$, required intermittent variety may be accomplished by the addition of a second medium having different permittivity values due their nature like dielectric, metal, or HMMs in its composition [14]. The study of PHCs includes both theoretical and experimental details [15, 16]. Studies in this area have also shown that, in contrast to HMMs, PHC structures exhibit a great potential for spontaneous emission

enhancement and efficient light outcoupling [17]. A surface electromagnetic wave (SEW) [18] is a type of electromagnetic wave that propagates along the surface of a material, rather than through the bulk of the material. SEWs are also sometimes referred to as surface plasmons or surface plasmon polaritons (SPP), depending on the nature of the wave [19]. Overall, the field of plasmonics and SPPs is rapidly evolving and expanding, with researchers continuing to develop new and innovative materials and devices with unique and exotic properties. As the field continues to mature, plasmonics and SPPs are likely to find new applications in a wide range of industries, from healthcare and energy to telecommunications and information technology. Theoretical study work by Ali [20–22] has examined the dispersion relations and wave propagation for TM nonlinear surface waves [23] and plasmon polariton gaps [24] in PHC. It has been shown that surface waves in a hypercrystal combine the characteristics of SPP at the metal–dielectric interface and Tamm states in the photonic crystal. As HMM exhibits various sorts of dispersion zones [25] in various frequency ranges, the resulting bands also display certain distinctive characteristics if the conditions of photonic gaps are met in these ranges. It has been demonstrated that the gaps in the frequency range where the PHC's HMM layer exhibits Type I behavior are red shifted, as opposed to the blue-shifted gaps of traditional PCs, meaning that they move to a lower frequency with increasing incidence angle. Here, we looked at how surface waves behaved inside these red-shifted gaps and compared it to how surface waves behaved inside blue-shifted gaps. Here, different PHCs are taken into account, and the characteristics of these surface waves as well as their reliance on certain structural elements are investigated.

2. Mathematical Formulism

Here we consider a PHC as shown schematically in Figure 1. It consists of a periodic dielectric layer of width d_d, permittivity ε_d, and a HMM layer of width d_H and dielectric permittivity tensor $\varepsilon_H = \begin{bmatrix} \varepsilon_d & 0 & 0 \\ 0 & \varepsilon_d & 0 \\ 0 & 0 & \varepsilon_d \end{bmatrix}$, Λ is the period of PHC as $\Lambda = d_H + d_d$.

According to the effective medium theory, the normal and transverse components of the HMM layer are as follows:

$$\varepsilon_\tau = p\varepsilon_m + (1-p)\varepsilon_d, \tag{1}$$

$$\varepsilon_n = \frac{1}{\frac{p}{\varepsilon_m} + \frac{1-p}{\varepsilon_d}}, \tag{2}$$

where $\varepsilon_m, \varepsilon_d, p$ represent, respectively, the permittivity of the metal layer, dielectric layer, and the filling factor of HMM defined as $= (d_m/(d_m + d_d))$. Rigorous coupled-wave analysis (RCWA) [26] is a semi-analytical method in computational electromagnetics that is most typically applied to solve scattering from the periodic dielectric structures. It is a Fourier-space method so devices and fields are represented as a sum of spatial harmonics. The field phasors in the region

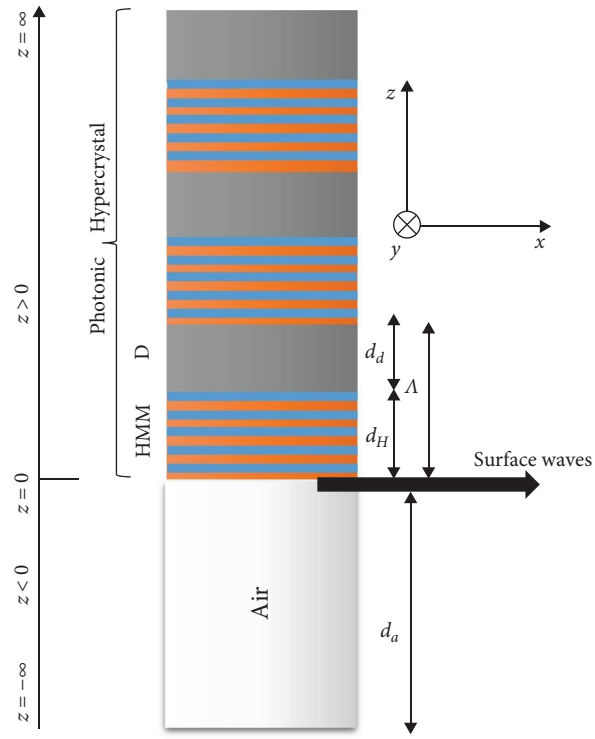

Figure 1: The schematic diagram of the photonic hypercrystal is ended with air. The surface wave propagates to x – axis in xy plane while the structure is designed along z – axis.

occupied by either partnering material are expressed as Fourier series with respect to x, just like the reflected and transmitted field phasors, q being the wave vector of the surface waves:

$$E(r) = \{e_x(z)u_x + e_y(z)u_y + e_z(z)u_z\}e^{iqx}, \tag{3}$$

$$H(r) = \{h_x(z)u_x + h_y(z)u_y + h_z(z)u_z\}e^{iqx}. \tag{4}$$

The Maxwell curl postulates ($\nabla \times E(r) = i\omega\mu_o H(r), \nabla \times H(r) = -i\omega\varepsilon\varepsilon_0 E(r)$) leads to a system of four ordinary differential equations that can be grouped into two cases: e_x, e_z, and h_y only for p-polarization (TM) and the other e_y, h_x, and h_z for s-polarization (TE), by eliminated $e_z(z)$ and $h_z(z)$ and combining them as a single matrix [27] equation given as follows:

$$\frac{d}{dz}\begin{bmatrix} e_x(z) \\ e_y(z) \\ h_x(z) \\ h_y(z) \end{bmatrix} = i\begin{bmatrix} \left(\omega\mu_0 - \frac{q^2}{\omega\varepsilon_\tau\varepsilon_0}\right)h_y(z) \\ (-\omega\mu_0)h_x(z) \\ \left(\frac{q^2}{\omega\mu_0} - \omega\varepsilon_n\varepsilon_0\right)e_y(z) \\ (-\omega\varepsilon_n\varepsilon_0)e_x(z) \end{bmatrix}. \tag{5}$$

Therefore, we can define for TE state $[f^{(s)}(z)] = [e_y(z)\eta_o h_x(z)]^T$ and TM state $[f^{(p)}(z)] = [e_x(z)\eta_o h_y(z)]^T$ using $\eta_o = \sqrt{\mu_0/\varepsilon_0}$, $\omega = k_o/\sqrt{\mu_0\varepsilon_0}$ and $k_o = \omega\sqrt{\mu_0\varepsilon_0}$ the

matrix differential equation is $d/dz\left[f^{(s,p)}(z)\right] = i\left[\underline{\underline{P}}^{(s,p)}(\beta, z)\right]\left[f^{(s,p)}(z)\right]$ for PHC where $z \in (0, \Lambda)$.

$$\left[\underline{\underline{Q_{\mathrm{PHC}}}}^{(s,p)}\right] = \left[\underline{\underline{W_{\mathrm{HMM}}}}^{(s,p)}\right].\left[\underline{\underline{W_d}}^{(s,p)}\right] = \begin{bmatrix} X_{11} & X_{12} \\ X_{21} & X_{22} \end{bmatrix}, \tag{6}$$

Where

$$\left[\underline{\underline{W_{\mathrm{HMM}}}}^{(p)}\right] = \exp\left\{i2\pi W \begin{bmatrix} 0 & \left(1 - \dfrac{Q^2}{\varepsilon_n}\right) \\ (\varepsilon_\tau) & 0 \end{bmatrix} D_1\right\},$$

$$\left[\underline{\underline{W_d}}^{(p)}\right] = \exp\left\{i2\pi W \begin{bmatrix} 0 & \left(1 - \dfrac{Q^2}{\varepsilon_d}\right) \\ (\varepsilon_d) & 0 \end{bmatrix} D_2\right\} \text{ and}$$

$$\left[\underline{\underline{W_{\mathrm{HMM}}}}^{(s)}\right] = \exp\left\{i2\pi W \begin{bmatrix} 0 & -(1) \\ (Q^2 - \varepsilon_\perp) & 0 \end{bmatrix} D_1\right\}, \quad \left[\underline{\underline{W_d}}^{(s)}\right]$$

$= \exp\left\{i2\pi W \begin{bmatrix} 0 & -(1) \\ (Q^2 - \varepsilon_{\mathrm{d}}) & 0 \end{bmatrix} D_2\right\}$. The electromagnetic field of the surface waves must diminish in magnitude as $z \longrightarrow \pm\infty$. Let $\left[V^{(s,p)}_{\mathrm{PHC,a}}\right]$ be the general eigen vector for both s and p polarized states corresponding to a general eigen value $\alpha^{(s,p)}_{\mathrm{PHC,a}}$. $\left[V^{(s,p)}_{\mathrm{PHC,a}}\right]$ be the eigen vector for PHC having eigen value $\alpha^{(s,p)}_{\mathrm{PHC,a}} = g$ such that $g > 0$.

$$\left[V^{(s,p)}_{\mathrm{PHC,a}}\right] = \begin{bmatrix} -\dfrac{X_{12}}{X_{11} - g} \\ 1 \end{bmatrix}. \tag{7}$$

For air eigen value $\alpha_a^{(s,p)} < 0$ thus $\alpha_a^{(s,p)} = -k_0\sqrt{(\varepsilon_a - Q^2)}$ and eigen vectors are, respectively, as follows:

$$\left[V_a{}^{(s)}\right] = \begin{bmatrix} \dfrac{1}{\sqrt{\varepsilon_a - Q^2}} \\ 1 \end{bmatrix}, \tag{8}$$

$$\left[V_a{}^{(p)}\right] = \begin{bmatrix} -\dfrac{\sqrt{\varepsilon_a - Q^2}}{\varepsilon_a} \\ 1 \end{bmatrix}. \tag{9}$$

The continuity of the field phasors required that $\left[f^{(s,p)}(0-)\right] = \left[f^{(s,p)}(0+)\right]$ where $\left[f^{(s,p)}(0-)\right] = \left[V_a{}^{(s,p)}\right] A_a^{(s,p)}$ and $\left[f^{(s,p)}(0+)\right] = \left[V^{(s,p)}_{PHC}\right] A_\Lambda^{(s,p)}$, $A_{\mathrm{a}}^{(s,p)}$, and $A_\Lambda^{(s,p)}$ are dimensionless scalars rearranged into the matrix equation as $\left[\underline{\underline{Y}}^{(s,p)}\right] = \left[-\left[V^{(s,p)}_{\mathrm{PHC}}\right]\left[V_a{}^{(s,p)}\right]\right]$ and for nontrivial solutions, the 2×2 matrices $\left[\underline{\underline{Y}}^{(s,p)}\right]$ must be singular, so that $\det\left[\underline{\underline{Y}}^{(s,p)}\right] = 0$.

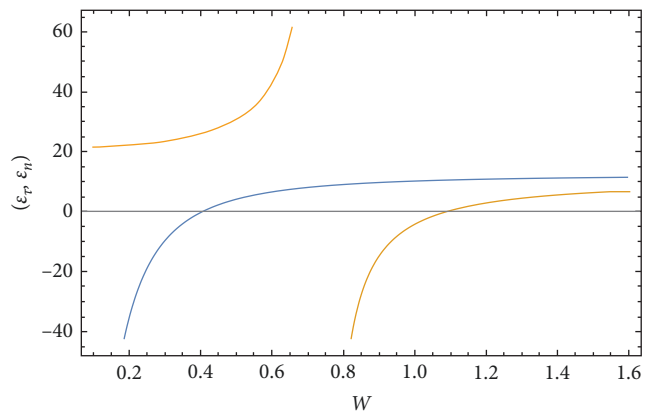

FIGURE 2: The plot of tangential ε_τ (blue) and normal ε_n (brown) components of dielectric constant for HMM versus de-dimensional frequency W.

$$1 + \left(\frac{X_{11} - g}{X_{12}}\right)\left(\frac{1}{\sqrt{\varepsilon_a - Q^2}}\right) = 0 \text{ (TE states)}, \tag{10}$$

$$1 - \left(\frac{X_{11} - g}{X_{12}}\right)\left(\frac{\sqrt{\varepsilon_a - Q^2}}{\varepsilon_a}\right) = 0 \text{ (TM states)}. \tag{11}$$

These are the dispersion relations for TE and TM polarization. The dispersion curves for the above surface states are obtained numerically and analyzed for different values of parameters as discussed below.

3. Results and Discussions

Now we apply our mathematical formulism to some specific set of parameters. we consider $Si/In:CdO$ as HMM and Si as dielectric material [28], here d_D and ε_d represent the width and permittivity of the dielectric layer and d_H represents the width of HMM layer consisting of Si and $In:CdO$ with layer width d_m and d_d, respectively. The electric permittivity of $In:CdO$ for lossless limit is $\varepsilon_m = \varepsilon_\infty + \omega^2/\omega_p^2$ where ε_∞ is high-frequency relative permittivity and ω_p is the plasma frequency. The de-dimensionalized parameters are defined as: width of HMM is $D_1 = d_H/\Lambda$ and that of dielectric layer is $D_1 = d_D/\Lambda$, angular frequency $W = \Lambda/\lambda_0$, and wave vector $Q = q/k_0$. The parameters and values used for the programing are as $d_D = 116.3$ nm width of silicon and $d_H = 252$ nm width of HMM, this HMM consists of four alternating layers of Si and $In:CdO$ mentioned as each of width $d_d = 44.1$ nm and $d_m = 18.9$ nm thus $d_H = 4\times(d_d + d_m) = 252$ nm. The PHC consist of HMM and dielectric medium having period $\Lambda = d_H + d_d = 368.3$ nm, also the plasma wavelength $\lambda_p = 899.34$ nm, plasma frequency $\omega_p = 2\pi c/\lambda_p = 2.09\times 10^{16} s^{-1}$, $\varepsilon_m = \varepsilon_\infty + \omega^2/\omega_p^2$, $\varepsilon_\infty = 5.5$, $\varepsilon_d = 14.98$, $\varepsilon_a = 1$, $p = 0.3$, $D_1 = 0.685$, and $D_2 = 0.315$. The dispersion curves of parallel (ε_τ) and perpendicular (ε_n) components of the HMM layer are shown in Figure 2.

Hence, there are four regions of interest on the frequency axis for HMM depending upon the different types of dispersion. For frequencies range $W > 0.01$ and $W < 0.4$ the values

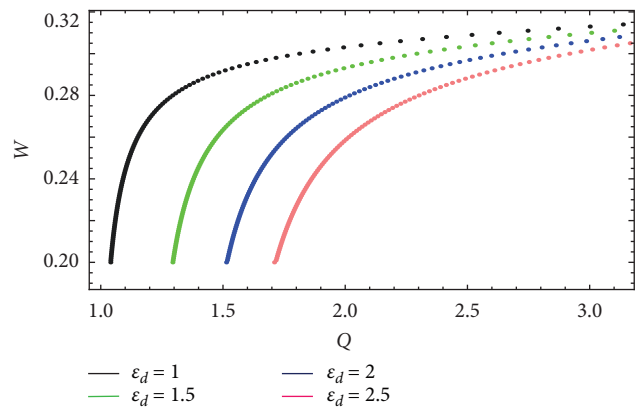

FIGURE 3: The dispersion curves of SPP for different interface dielectric materials in the Type II region of HMM.

of normal and transverse components of the permittivity tensor are as $\varepsilon_\tau < 0, \varepsilon_n > 0$ so that HMM is of Type II, and for frequencies $W > 0.4$ and $W < 0.8$ both dielectric components are positive $\varepsilon_\tau > 0, \varepsilon_n > 0$ showing the anisotropric nature of HMM material, whereas for frequencies range $W > 0.8$ and $W < 1.1 \varepsilon_\tau > 0, \varepsilon_n < 0$ the HMM is of Type I, and for frequencies $W > 0.8$ again both dielectric components are positive $\varepsilon_\tau > 0, \varepsilon_n > 0$ showing anisotropic nature of HMM material. In the frequency region where the HMM shows Type II behavior, all the conditions to excite the surface plasmon polariton (SPP) for TM incident radiation are met. Figure 3 shows the corresponding dispersion curves for different interface dielectric media. With increasing values of the permittivity of the interface medium, the wavevectors of the SPP shift toward higher values implying more subwavelength confinement and tend to approach the same SPP resonance frequency. This is the same behavior as in the case of SPP at metal–dielectric interface. The advantage here is that the SPP resonance frequency can be engineered as desired by the choice of the filling factor of the HMM layer and other parameters of the PHC [28].

When we consider the wave propagation through a finite periodic structure (the PHC under consideration for the given parameters) and the conditions for a Bragg gap in Type I region are satisfied, this gap shows a red shift in frequency as the angle of incidence is increased for $\theta = 0\pi$, $(\pi/6)$, and $(\pi/3)$, as shown in Figure 4(a). For TE polarized incident light, the gap shows the normal blue shift of frequency with increasing angle of incidence (Figure 4(b)), as the structure behaves as a regular photonic crystal rather than a PHC.

The red shift and blue shift of the gaps in the Type I dispersion region of HMM are already well explained in the literature by Xia et al [16] and can be summarized in the following way: the existence of the Bragg gap implies the satisfaction of the following condition on the phase

$$\varphi = (k_H)_z d_H + (k_D)_z d_D = n\pi, \tag{12}$$

$$\frac{d\varphi}{dk_x} = \frac{d(k_H)_z}{dk_x} d_H + \frac{dy}{dk_x} d_D. \tag{13}$$

In conventional PCs, both layers of the periodic structure are dielectric with iso-frequency curves in the wavevector space being spheres for which $dk_z/dk_x < 0$ are shown in Figure 5(a), where $k_x = k \sin\theta$, so with increasing incident angle the gap is blue shifted on the frequency axis. In the structure considered here, the HMM layer shows (Figure 5(b)) the hyperbolic dispersion of iso-frequency curves in the wavevector space for Type I region for which $dk_z/dk_x > 0$, so that it may happen that $d\varphi/dk_x > 0$, and gap becomes red shifted with the frequency axis [28]. Here, these gaps are located merely by numerical exploration.

This polarization-dependent shifting of the gap on the frequency axis effects the nature of the surface waves that decay inside this gap. Figure 6(a) shows the dispersion plot of the surface waves when the periodic structure is a PHC, i.e., the incident light is p-polarised. The vertical axis represents the dimensionless frequency W, whereas the horizontal axis represents the dimensionless wave vector Q. The negative slope [29] of the dispersion curve represents the group velocity dW/dQ being negative. The surface waves are left-handed. This is in fact the direct consequence of the red shift of the gap inside which the SW is decaying. The increasing the value of Q on the horizontal axis represents the increasing value of the incidence angle for a given value of the incident frequency. As the gap is shifted, so is the frequency. It means an increase in Q value is accompanied by a decrease in W value in the dispersion curve of the surface waves. Figure 6(b) shows the dependence of these dispersion curves on the dielectric constant of the interface medium. As the dielectric constant increases, shown in Figure 6(b) (b1, b2, and b3), i.e., $\varepsilon_d = 1, 1.5,$ and 2, the wave vector Q is shifted higher on the frequency axis above 0.94, and the group velocity is positive but decreasing. It is significant to keep in mind that the group velocity is distinct from the phase velocity, which is the rate of a wave's phase propagation. The group velocity, which determines how quickly the wave's energy spreads, depends on a number of variables, including the properties of the medium the wave travels through. The refractive index of the medium at the interface between the two materials will vary when two different dielectric materials are brought into contact with one another. As a result, the SW group velocity changes, varying the SW speed and direction. When dielectric materials with increasing dielectric constants are in contact with PHC, the group velocity decreases as the ε_d values rise because for $\varepsilon_d = 1$ more refraction and less time to pass the interface increase the group velocity, whereas for $\varepsilon_d = 1.5$ or 2 less refraction results in more time to pass the interface, which causes the group velocity to fall. The behavior is just opposite in the cases of Figures 7(a) and 7(b) for the interface of PHC with air and then with different dielectric materials with increasing dielectric constants, i.e., $\varepsilon_d = 1, 1.5,$ and 2, when the incident light polarization is TE and the periodic structure is just a

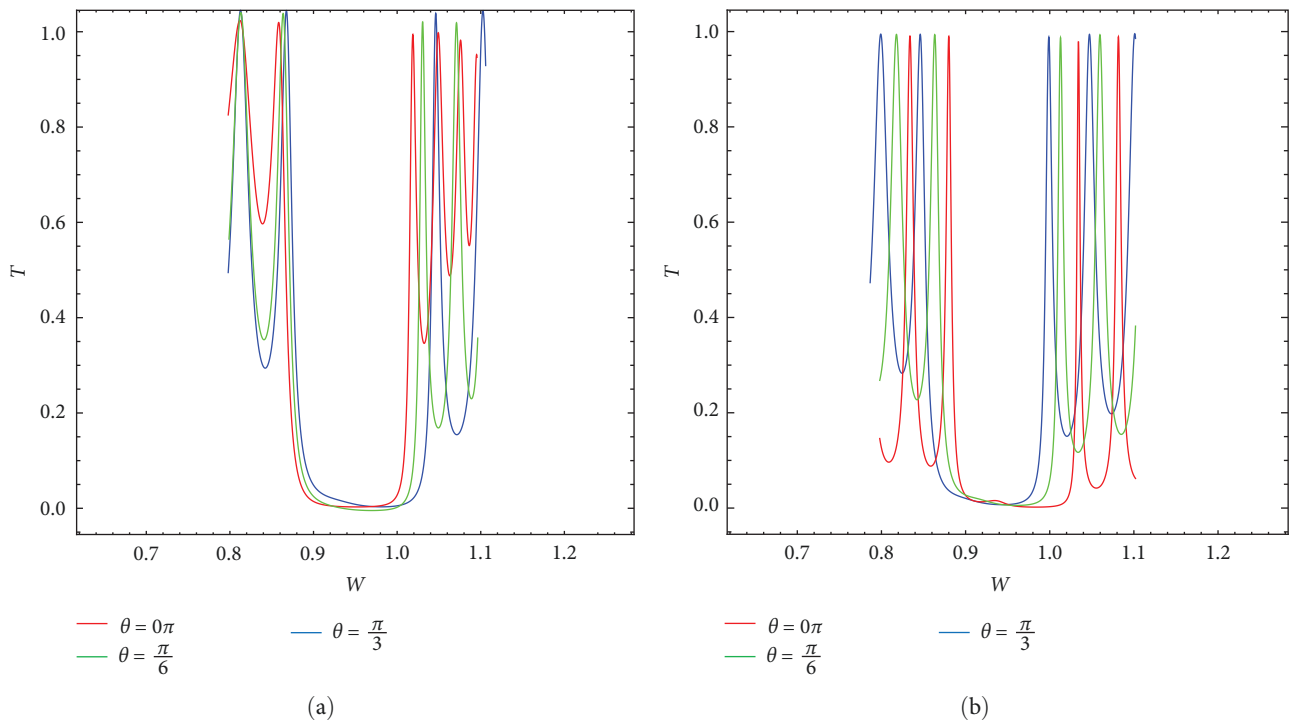

Figure 4: (a) The plot of transmittance T and de-dimensional frequency W, shows red shift with increasing angle of incident in Type I HMM for TM polarization. (b) The plot of transmittance T and de-dimensional frequency W, shows blue shift with increasing angle of incident in Type I HMM for TE polarization.

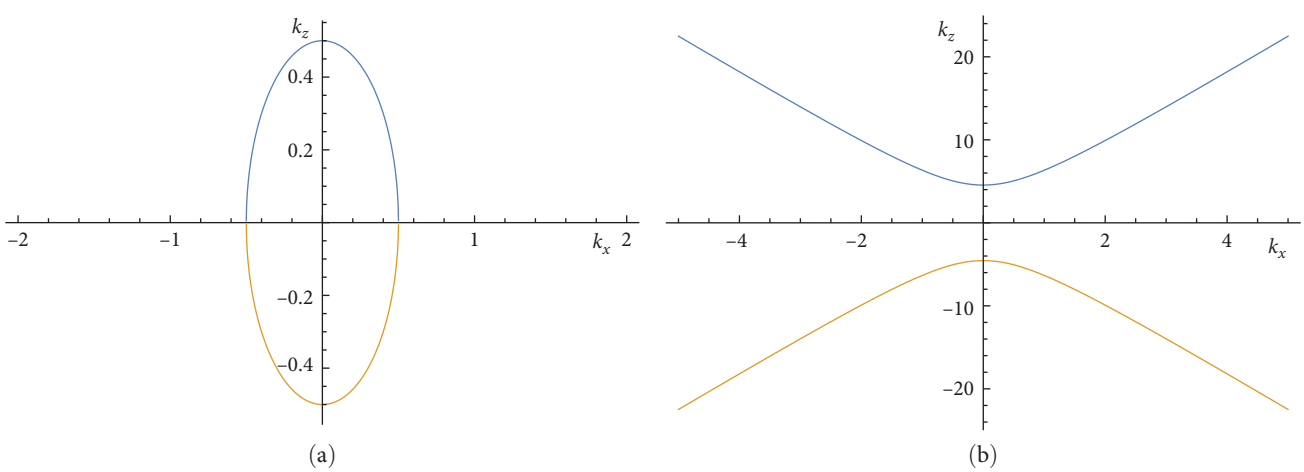

Figure 5: (a) The plot shows iso-frequency curves in wavevector k_z and k_x for Regions II and IV of HMM. (b) The plot of wavevector k_z and k_x for Region III shows Type I HMM.

conventional photonic crystal. An increase in Q value can be treated as an increase in the incident angle for a fixed incident frequency that is blue shifted in this case and hence accompanied by the increase in frequency. Resultantly, the dispersion curve shows right-handedness in the group velocity.

The group velocity for TE mode is shown by the dispersion plots to be positively increasing for air; however, as the dielectric constant increases at the interface of PHC and dielectric materials, the slope indicates that the group velocity is decreasing. Higher dielectric constants result in materials taking longer to pass through the interface, reducing refraction. For TM polarization, the plots reveal that the group velocity of SPP waves for HMM of Type I is positive and negative but decreasing for PHC, the propagating light may be "backward propagating" if the dispersion curve has a negative slope. We show that depending on the configurations, the same photonic (plasmonic) system can support both positive and negative group velocities. The highly active field of "negative index" metamaterials, in which the pulse group and power propagate in the same direction while the phase velocity is antiparallel, frequently asserts that the negative group

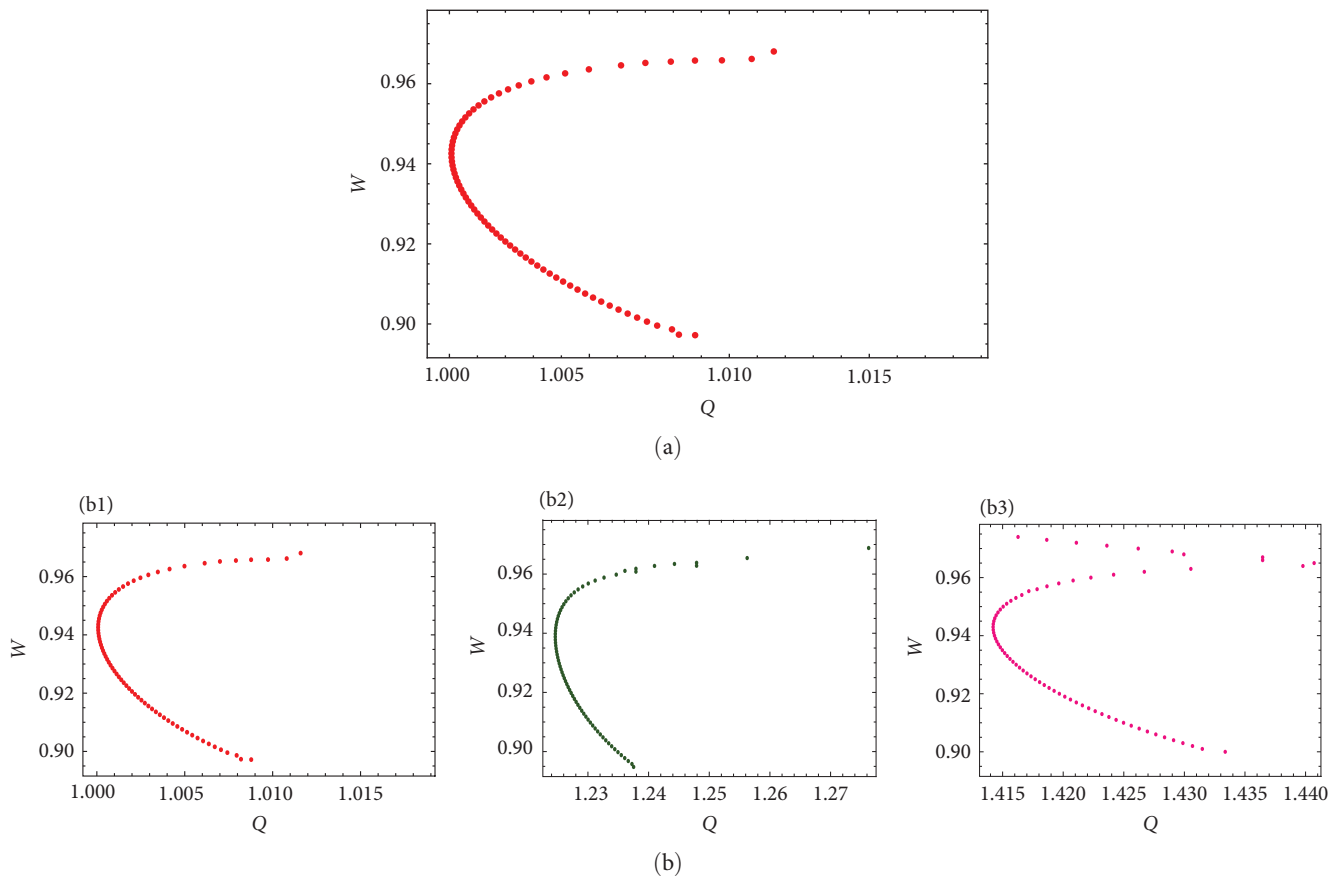

Figure 6: (a) The plot of de-dimensional frequency W and wavevector Q, shows red shift assuming interface of PHC with air in p-polarisation. (b) The plots of de-dimensional frequency W and wavevector Q, confirm red shift at interface of PHC with dielectric metarials of different ε_d in p-polarisation.

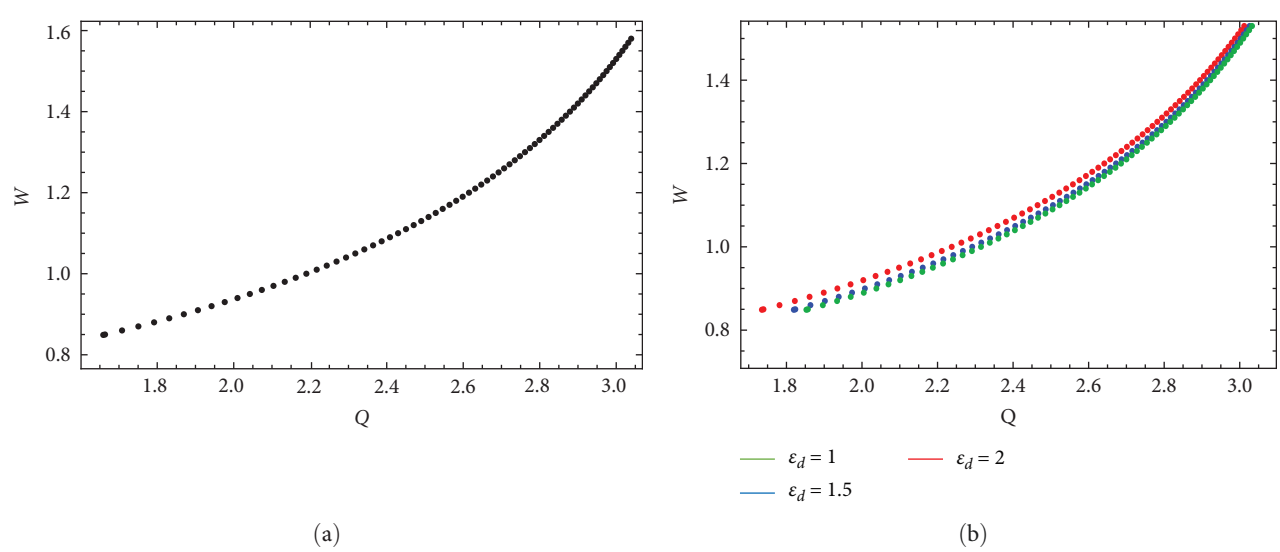

Figure 7: (a) The plot of de-dimensional frequency W and wavevector Q, shows blue shift assuming interface of PHC with air in s-polarization. (b) The plot of de-dimensional frequency W and wavevector Q, confirm blue shift assuming the interface of PHC with dielectric material of different constant ε_d in s-polarization.

velocity suggests negative refraction. The corresponding SPP are characterized by the wave vectors, group velocity, and a very small decay length. The frequency depends essentially on the permittivity of the dielectric, and the plasma frequency of the metal. Further investigation may be done by including the nonlinearities in this problem and their dispersion plots which can explain their propagation for SPP.

4. Concluding Remarks

The dispersion relation of linear surface waves in PHC is explored, and the results are extended using Mathematica and RCWA. We observed that SPP are red shifted and blue shifted for TM and TE waves as the incident angle increases for Type I HMM, also SW are left-handed with decreasing positive and negative group velocity for TM mode and right-handed with increasing positive group velocity for TE mode. Further, the combined effect of anisotropic material and the PHC can also be examined for understanding more about how surface waves propagate. There are several limitations and challenges associated with SPP waves in PHCs such as dispersion and band gap engineering, losses and damping, fabrication challenges, coupling efficiency, limited tunability, and polarization sensitivity. The decay of surface red shifts and blue shifts band gaps for PHC is discussed here for the first time. Furthermore, nonlinear effects of these PHC for red-shifted and blue-shifted band gaps can be discussed, and gap solitons can also be explored. Additionally, the nonlinearity prevents infinite wavevector divergence for such PHC surface waves. It is anticipated that this early research will serve as the foundation for PHC in the future, allowing nonlinearity to be used to investigate more unique properties of these structures.

Data Availability

The data used to support the findings of this study are available from the corresponding author upon request.

Conflicts of Interest

The authors declare that they have no conflicts of interest.

References

[1] E. E. Narimanov, "Photonic hypercrystals," *Physical Review X*, vol. 4, no. 4, Article ID 041014, 2014.

[2] P. Yeh, A. Yariv, and C. S. Hong, "Electromagnetic propagation in periodic stratified media. I. General theory," *Journal of the Optical Society of America*, vol. 67, no. 4, pp. 423–438, 1977.

[3] M. Kim, S. Kim, and S. Kim, "Optical bistability based on hyperbolic metamaterials," *Optics Express*, vol. 26, no. 9, pp. 11620–11632, 2018.

[4] Z. Huang and E. E. Narimanov, "Optical imaging by photonic hyper-crystal: veselago lens and beyond," *Journal of Optics*, vol. 16, no. 11, Article ID 114009, 2014.

[5] E. Yablonovitch, "Inhibited spontaneous emission in solid-state physics and electronics," *Physical Review Letters*, vol. 58, no. 20, pp. 2059–2062, 1987.

[6] S. John, "Strong localization of photons in certain disordered dielectric superlattices," *Physical Review Letters*, vol. 58, no. 23, pp. 2486–2489, 1987.

[7] G. Naik and A. Boltasseva, "Plasmonics and metamaterials: looking beyond gold and silver," *SPIE Newsroom*, 2012.

[8] E. Reyes-Gómez, D. Mogilevtsev, S. B. Cavalcanti, C. A. A. de Carvalho, and L. E. Oliveira, "Plasmon polaritons in photonic superlattices containing a left-handed material," *Europhysics Letters*, vol. 88, no. 2, Article ID 24002, 2009.

[9] P. Shekhar, J. Atkinson, and Z. Jacob, "Hyperbolic metamaterials: fundamentals and applications." *Nano Convergence*, vol. 1, Article ID 14, 2014.

[10] V. A. Podolskiy and E. E. Narimanov, "Strongly anisotropic waveguide as a nonmagnetic left-handed system," *Physical Review B*, vol. 71, no. 20, Article ID 201101, 2005.

[11] Z. Jacob and E. E. Narimanov, "Optical hyperspace for plasmons: dyakonov states in metamaterials," *Applied Physics Letters*, vol. 93, no. 22, Article ID 221109, 2008.

[12] Y. Guo, C. L. Cortes, S. Molesky, and Z. Jacob, "Broadband super-planckian thermal emission from hyperbolic metamaterials," *Applied Physics Letters*, vol. 101, no. 13, Article ID 131106, 2012.

[13] E. E. Narimanov, "Dirac dispersion in photonic hypercrystals," *Faraday Discussions*, vol. 178, pp. 45–59, 2015.

[14] M. Z. Ali, A. A. Bhatti, Q. ul Haque, and S. Mahmood, "Global transmission diagrams for evanescent waves in a nonlinear hyperbolic metamaterial," *Chinese Optics Letters*, vol. 13, no. 9, Article ID 090601, 2015.

[15] B. Janaszek and P. Szczepanski, "Distributed feedback laser based on tunable photonic hypercrystal," *Materials*, vol. 14, no. 15, Article ID 4065, 2021.

[16] J. Xia, Y. Chen, and Y. Xiang, "Enhanced spin hall effect due to the redshift gaps of photonic hypercrystals," *Optics Express*, vol. 29, no. 8, pp. 12160–12168, 2021.

[17] A. Moradi, "Electrostatic waves in photonic hypercrystals," *Physics Letters A*, vol. 387, Article ID 127008, 2021.

[18] R. H. Ritchie, "Plasma losses by fast electrons in thin films," *Physical Review*, vol. 106, no. 5, pp. 874–881, 1957.

[19] S. A. Maier, *Plasmonics: Fundamentals and Applications*, Springer, 2007.

[20] M. Z. Ali, "Nonlinear surface waves in photonic hypercrystals," *Physics Letters A*, vol. 381, no. 32, pp. 2643–2647, 2017.

[21] M. Z. Ali, "Dispersion relations and wave propagation in photonic hypercrystals," *Modern Physics Letters B*, vol. 32, no. 2, Article ID 1750320, 2018.

[22] M. Z. Ali, "Plasmon-polariton gap and associated phenomenon of optical bistability in photonic hypercrystals," *Physics Letters A*, vol. 387, Article ID 127026, 2021.

[23] Z. Shi, G. Piredda, A. C. Liapis, M. A. Nelson, L. Novotny, and R. W. Boyd, "Surface plasmon polaritons on metal-dielectric nanocomposite films," *Optics Letters*, vol. 34, no. 22, pp. 3535–3537, 2009.

[24] S. Kurilkina, V. Belyi, and N. Kazak, "Surface plasmon-polaritons at the Interface of magnetoelectric hyperbolic metamaterial," *Nonlinear Phenomena in Complex Systems*, vol. 23, no. 3, pp. 327–331, 2020.

[25] Q. Anh, N. Pham, and N. N. Hieu, "Surface plasmon-polaritons in anisotropic hyperbolic metamaterials," *Journal of Nonlinear Optical Physics & Materials*, vol. 32, no. 2, Article ID 2350012, 2023.

[26] M. Lax and D. F. Nelson, "Maxwell equations in material form," *Physical Review B*, vol. 13, no. 4, pp. 1777–1784, 1976.

[27] J. Polo, T. Mackay, and A. Lakhtakia, *Electromagnetic Surface Waves: A Modern Perspective*, Elsevier, Amsterdam, 2013.

[28] F. Wu, S. Xiao, D. Liu, Z. Chen, G. Chen, and X. Peng, "Complete redshift photonic bandgap and dual wavelength polarization selection in periodic multilayer structure containing hyperbolic metamaterial," *Optics Communications*, vol. 495, Article ID 127117, 2021.

[29] E. Feigenbaum, N. Kaminski, and M. Orenstein, "Negative dispersion: a backward wave or fast light? Nanoplasmonic example," *Optics Express*, vol. 17, no. 21, pp. 18934–18939, 2009.